Journal of Hazardous Materials 184 (2010) 73–80

Contents lists available at ScienceDirect

Journal of Hazardous Materials

journal homepage: www.elsevier.com/locate/jhazmat

The impact of zero-valent iron nanoparticles on a river water bacterial community

Robert J. Barnes[a], Christopher J. van der Gast[b], Olga Riba[c], Laura E. Lehtovirta[d], James I. Prosser[d], Peter J. Dobson[e], Ian P. Thompson[a,*]

[a] Department of Engineering Science, University of Oxford, Parks Road, OX1 3PJ, UK
[b] Centre for Ecology and Hydrology, Mansfield Road, Oxford, OX1 3SR, UK
[c] Interface Analysis Centre, University of Bristol, 121 St. Michael's Hill, Bristol BS2 8BS, UK
[d] Institute of Biological and Environmental Sciences, University of Aberdeen, St. Machar Drive, AB24 3UU, UK
[e] Begbroke Directorate, Oxford University Begbroke Science Park, Sandy Lane, OX5 1PF, UK

ARTICLE INFO

Article history:
Received 2 June 2010
Received in revised form 20 July 2010
Accepted 2 August 2010
Available online 8 August 2010

Keywords:
Zero-valent iron nanoparticles
River water
Bacterial community
Richness
Recovery

ABSTRACT

Zero-valent iron (ZVI) nanoparticles are of interest because of their many potential biomedical and environmental applications. However, these particles have recently been reported to be cytotoxic to bacterial cells. The overall objective of this study was to determine the impact of 100 mg/L ZVI nanoparticles on the diversity and structure of an indigenous river water bacterial community. Response during exposure for 36 days was determined by denaturing gel gradient electrophoresis (DGGE) analysis of bacterial 16S rRNA genes, amplified from extracted DNA, and viable and total cell abundances were determined by plate counting and fluorescent microscopy of DAPI-stained cells. Changes in river water chemistry were also monitored. Addition of ZVI nanoparticles led to a rapid decrease in oxidation–reduction potential (ORP) (+196 to −281 mV) and dissolved oxygen (DO) concentration (8.2–0.6 mg/L), both of which stabilized during the experiment. Interestingly, both viable and total bacterial cell abundances increased and pH decreased, characteristic of an active microbial community. Total community structure was visualized using rank-abundance plots fitted with linear regression models. The slopes of the regression models were used as a descriptive statistic of changes in evenness over time. Importantly, despite bacterial growth, addition of ZVI nanoparticles did not influence bacterial community structure.

1. Introduction

Zero-valent iron (ZVI) nanoparticles, characterized by high surface areas and reactivity, are of interest because of their potential applications in catalysis, magnetism, electronics and biomedical and environmental engineering [1]. An important application of these particles is subsurface injection for the remediation of groundwater contaminated with chlorinated aliphatic hydrocarbons (CAHs) [2–4]. The employment of ZVI nanoparticles for waste water disinfection has also been proposed [5]. Unlike many other nanomaterials, which may accidentally enter the environment, large concentrations of ZVI nanoparticles may be intentionally released. Research on ecotoxicity is therefore needed to assess increasing concerns regarding the environmental use of such nanomaterials and to minimise any unintended impact. There is little information on the microbial toxicity of ZVI nanoparticles and published studies are restricted to investigations of effects on single bacterial strains [5–7], rather than on microbial communities, and of only short-term exposure (5 min or 1 h) in sterile deionised water or Phosphate Buffered Saline (PBS). For example, Lee et al. [6] found that <100 mg/L ZVI nanoparticles rapidly inactivated *Escherichia coli* (*E. coli*) cells, with significant physical disruption of the cell membranes and subsequent leakage of intracellular contents from exposed cells. They proposed that this disturbance of cell integrity resulted in inactivation or enhanced the biocidal effects of dissolved iron. In addition, the reaction of Fe (II) with intracellular hydrogen peroxide (Fenton reaction) or oxygen may have induced oxidative stress by producing reactive oxygen species (ROS). These findings concur with Auffan et al. [7], who showed that ZVI nanoparticles at concentrations <100 mg/L were cytotoxic to *E. coli* cells, and suggested that this was due to oxidative stress. This stress resulted from the generation of ROS from the Fenton reaction during the oxidation of ZVI nanoparticles to magnetite. This finding was directly supported by increased sensitivity in superoxide dismutase (SOD) deficient *E. coli* cells as, without this enzyme, the cells had limited defence against oxidative stress. Other potential toxicity mechanisms were disruption of membrane integrity, or disturbance of the

* Corresponding author. Tel.: +44 (0) 1865 283789; fax: +44 (0) 1865 374992.
E-mail address: Ian.Thompson@eng.ox.ac.uk (I.P. Thompson).

0304-3894/$ – see front matter © 2010 Elsevier B.V. All rights reserved.
doi:10.1016/j.jhazmat.2010.08.006

cell electron and ionic transport chains through strong adsorption of oxidizing ZVI nanoparticles to the bacterial cell wall [7]. Diao and Yao [5] showed that 100 mg/L ZVI nanoparticles rapidly inactivated *Pseudomonas fluorescens* and *Bacillus subtilis* var. *niger* cells. Gram-positive cells were more resistant than Gram-negative cells, with greater doses of ZVI nanoparticles required for complete inactivation [5]. The observed cell inactivation was attributed to physical coating by the ZVI nanoparticles, disruption of cell membranes and generation of ROS.

These results highlight the particular care that must be taken to understand fully the potential ecotoxicological impacts of these materials, given their increasing use in environmental and manufacturing applications. Consequently, the major objective of this study was to determine the impact of ZVI nanoparticles on the diversity and structure of a natural bacterial community in river water. River water was selected as a model system for studying the effects of ZVI nanoparticles upon bacterial communities as rivers are accessible and common natural ecosystems that support a diverse array of aquatic organisms. Furthermore, nanoparticles released into the environment are likely to accumulate in river and groundwaters.

2. Materials and methods

2.1. Reagents and synthesis of ZVI nanoparticles

The $FeSO_4{\cdot}7H_2O$, $NaBH_4$(s), ethanol and acetone used in this study were of analytical grade. ZVI microparticles (>99.5%) were manufactured by Alfa Aesar (product no. 00170). ZVI nanoparticles were synthesized via reductive precipitation, as previously described [8].

2.2. Establishment and sampling of river water microcosms

Samples of river water were taken from a section of the River Thames bordering Port Meadow, near Wolvercote, Oxfordshire (UK National Grid Reference: SP495083), on 14th November, 2008. Samples were collected from the middle of the river channel at a depth of approximately 0.5 m.

Microcosms were prepared by adding 10 L of river water to an autoclaved (121 °C for 15 min) bottle [SciLabware, Stone, UK (product no. BNP10B)]. This volume enabled 250 ml of river water to be extracted at each sample point (total removal = <20% of initial volume), the quantity required for strong DNA product (data not shown). Three different experimental conditions were established: river water, river water plus 100 mg/L ZVI microparticles and river water plus 100 mg/L ZVI nanoparticles, with three replicates for each treatment. Sterile microcosms (with and without nanoparticles) were also set up as controls. River water was sterilized by autoclaving three times at 121 °C for 15 min, with 24 h between each run. River water microcosms were sampled before addition of the ZVI particles and after incubation for 1, 3, 6, 11, 21 and 36 days at a constant temperature of 20 °C, with daily mixing of river water and particles by shaking for 1 min.

2.3. Analysis of ZVI particles and water chemistry

Fe, S, B and Na particle contents were determined using a Thermo-Finnigan Element 2 High-Resolution Inductively Coupled Plasma Mass Spectrometer (HR-ICP-MS).

X-ray Photoelectron Spectroscopy (XPS) analysis was performed using a Thermo VG Scientific Escascope, equipped with a dual anode X-ray source (AlKα 1486.6 eV and MgKα 1253.6 eV), as previously described [8].

X-Ray Diffraction (XRD) was carried out using a Phillips Xpert Pro diffractometer with a CuKα source, as previously described [8]. MacDiff software version 4.2.5 (Petschick, 2001) was used to display diffractograms and to identify the minerals.

Transmission Electron Microscope (TEM) images and diffraction patterns were obtained with a Philips 430 TEM operating at 250 kV.

A Focused Ion Beam (FIB) (FEI Strata 201, Hillsboro, USA) was used to image the ZVI particles. The resolution of the system is dependent on the operating conditions. At 30 kV, the resolution was 500 nm for an operating current above 11 pA and at least 5–7 nm for a current of 1 pA. Secondary electrons released from ion beam sputtering were detected by a channeltron electron multiplier. As the etch rate of the surface is proportional to beam current, a low beam current was usually chosen to minimise etching during imaging.

Particle size distribution was measured using a CPS Disc Centrifuge (Model DC24000, CPS Instruments, Inc., New Town, USA), as previously described [8], but with no sonication step and a maximum operation speed of 10,000 rpm. In addition to analysis of ZVI particles, river water was centrifuged to concentrate colloidal particles for size analysis.

BET specific surface area was measured using the nitrogen adsorption method (5 point isotherm) with a Gemini VI Surface Area and Pore Size Analyzer (Micromeritics, Norcross, USA).

River water pH (INTELLICAL pH standard electrode, liquid electrolyte), oxidation–reduction potential (ORP) (Redox radiometer electrode) and dissolved oxygen (DO) concentration (INTELLICAL LDO standard sensor) were measured using a HQ30d Portable Meter (Hach Lange, Manchester, UK). The probes were washed with 70% (v/v) ethanol between each microcosm analysis to avoid cross-contamination.

2.4. Bacterial enumeration

The total number of bacteria was determined by staining cells with 4′,6-diamidino-2-phenylindole (DAPI), according to Saby et al. [9] with minor modifications. In brief, 10 ml of sample was placed in a sterilized amber glass vial containing 1 ml DAPI (0.5 μg/ml) and 1 ml Triton X-100 (0.1%), both filter-sterilized through cellulose nitrate filters (pore size 0.2 μm). Samples were mixed for 30 s, left to stand for 10 min and filtered through black polycarbonate filters. Filters were rinsed twice with 15 ml of bacterium-free distilled water and allowed to air dry. Once dry, 20 μl of SlowFade® Gold antifade reagent (Invitrogen, Paisley, UK) was pipetted onto the centre of the filter and covered with a cover slip. The filters were examined under UV light with an epifluorescence microscope (Nikon Eclipse E400, Amstelveen, The Netherlands) and an oil immersion objective. Viable heterotrophic counts were determined by spread plating, in triplicate, 100 μl of undiluted sample and 10^{-1}, 10^{-2} and 10^{-3} dilutions on Nutrient Agar (Oxoid, Basingstoke, UK). Plates were incubated at 20 °C (±2 °C) for 10 days, when colonies were counted. Viable cell abundances are expressed as colony forming units (CFUs) per ml.

2.5. Extraction of DNA and DGGE analysis

Microcosm river water (250 ml) was pre-filtered (20 μm pore size) and subsequently filtered on hydrophilic filters [ME 24/21 ST (pore size, 0.2 μm; diameter, 47 mm); Whatman, Maidstone, UK]. Bulk genomic DNA was extracted using sodium dodecyl sulphate (SDS) hexadecyltrimethyl ammonium bromide (CTAB) [10] and products were examined by agarose (1% w/v) gel electrophoresis in Tris/borate/EDTA buffer (TBE).

For denaturing gradient gel electrophoresis (DGGE) analyses, a 192-base-pair fragment of the 16S rRNA gene was amplified from diluted (1/10) genomic DNA extracts by PCR using universal bacterial primers targeting the V3 region. The forward primer (GC338F), including an adjoining 39-base-pair GC clamp, consisted of the sequence 5′-CGCCCGCCGCGCCCCCGCCCCGGCCC-

GCCGCCCCCGCCCACTCCTACGGGAGGCAGC-3′, and the reverse primer (530R) sequence was 5′-GTATTACCGCGGCTGCTG-3′ [11]. Primers were synthesized by Thermo Fisher Scientific (Loughborough, UK). Each 50 μl PCR mixture comprised 1× $MgCl_2$-free buffer, 1 mM dNTPs, 400 nM forward primer, 400 nM reverse primer, 2 mM $MgCl_2$, 20 ng BSA, 1 U *Taq* DNA polymerase (Bioline, London, UK) and 1 μl template DNA. The PCR amplifications were performed using a Px2 Thermal Cycler (Thermo Fisher Scientific, Loughborough, UK) as follows: initial denaturation of 95 °C for 5 min followed by 10 cycles of 94 °C for 30 s, 55 °C for 30 s, 72 °C for 30 s, followed by 25 cycles of 92 °C for 30 s, 55 °C for 30 s, 72 °C for 40 s, followed by final extension at 72 °C for 10 min. After PCR, the BSA was removed from each sample product using maXtract™ high density tubes (Qiagen, Crawley, UK) with phenol:chloroform (1:1) and chloroform solutions. Amplification products were examined by agarose (1.5% w/v) gel electrophoresis in Tris–acetate–EDTA buffer (TAE). The cleaned PCR products were loaded onto an 8% (w/v) acrylamide gel in 0.5× TAE buffer containing a 35–70% denaturing gradient. The denaturing gradient gel was prepared by mixing zero and 80% denaturant solutions, 80% denaturant consisting of 5.6 M urea and 32% (v/v) formamide. All gels were cast using the Gilson Minipuls 3 system (Anachem, Luton, UK). Gels were electrophoresed at 60 °C at a constant voltage of 75 V for 16 h using the DCode™ Universal Mutation Detection System (Bio-Rad, Hemel Hempstead, UK). Gels were subsequently silver-stained, as previously described [12]. DGGE band and profile analyses were performed using Phoretix 1D Advanced software (Nonlinear Dynamics Ltd., Newcastle upon Tyne, UK) and the number and intensity of bands were used to infer estimates of taxon richness and relative abundance as previously described and discussed [10,13].

2.6. Statistical analysis of data

Rank-abundance plots were used to determine differences in bacterial community structure [14]. For each sample the relative abundance of each taxon (DGGE band) was standardized to normalized percent values before construction of the rank-abundance plots. The rank-abundance plots were visualized by plotting relative abundance (log_{10} transformed) versus taxa rank order. A linear regression model was fitted for each plot and the regression slope value was used as a descriptive statistic for changes in community structure. Linear regressions, coefficients of determination (r^2) and significance (P) were calculated using Minitab software (version 14.20, Minitab, University Park, PA). Community composition was compared using the Sørenson index of similarity, $S_{SOR} = 2a/2a + b$, were a is the number of co-occurring taxa in two given samples and b is the total number of taxa occurring in one sample only. S_{SOR} was generated using the PAST (Palaeontological statistics program, version 1.90, http://folk.uio.no/ohammer/past). Differences in community composition and taxon richness before and after treatment were performed using one-way analysis of variance (ANOVA) tests using Minitab software. Taxon–time relationships were analyzed as previously described [13], power law regressions, coefficients of determination (r^2), and significance values were calculated using Minitab software and the t-distribution method was used to compare the regression line slopes as described in [15].

3. Results and discussion

3.1. Iron particle characterization

TEM images showed ZVI nanoparticles to be 30–90 nm in diameter with spherical or pseudo-spherical forms, while diffraction contrasting revealed the particle cores to be polycrystalline with metal crystals <3 nm across. Dried particles aggregated into chains, possibly due to magnetic interactions between the primary metal particles [16]. Nanoparticles were covered by an amorphous, low density outer layer of uniform thickness (3–4 nm) ascribed to surface oxide. Analysis of diffraction patterns recorded from the metallic core indicated a body centred cubic (bcc) crystalline structure characteristic of α-Fe. Focused Ion Beam (FIB) images indicated the presence of larger spherical particles, ranging from 40 to 150 nm (Fig. 1A and B), and aggregation of particles into chains. ZVI microparticles purchased from Alfa Aesar showed particles of 2–3 μm in diameter (TEM) or 1.5–6.5 μm (FIB) with no obvious oxide shell (TEM), as the particle thickness prevented transmission of the beam through particles, and no aggregation was observed (FIB imaging) (Fig. 1C and D).

Particle size distribution analyzed by weight is presented in Table 1. Magnetic interactions between the primary metal particles caused a significant (>80%) aggregation of nanoparticles, giving a combined diameter >150 nm. Aggregation was exacerbated by disc centrifuge analysis, which analyzed particles that had been added to water, leading to greater agglomeration [17]. Enhanced aggregation of ZVI nanoparticles in solution and the influence of pH on colloidal stability were also noted by Auffan et al. [7]. In Milli-Q™ water, ZVI nanoparticles ranged from 0 to 2794 nm, mean = 457.3 nm. In comparison ZVI microparticles ranged from 279 nm to 10.07 μm, mean = 3.95 μm. The size distribution of ZVI nanoparticles changed when added to river water (Table 1), but resulted in a very similar average particle size (460.1 nm), and showed the true combined diameter of the aggregated particles when present in the river water used in this study. Colloidal particles of a range of compounds naturally occurring in the river water ranged from 0 to 3925 nm (mean = 860.8 nm).

Due to their small size, the ZVI nanoparticles had a BET specific surface area of 18.3 m^2/g, significantly higher than that of the ZVI microparticles (0.37 m^2/g).

Table 1
Size distribution of particles by weight (% fraction), determined by CPS Disc Centrifuge. ZVI nanoparticles and river water colloidal particles analyzed at 10,000 rpm. ZVI microparticles analyzed at 2500 rpm.

Material	0–47 nm	47–150 nm	150–270 nm	270–484 nm	484–868 nm	868–2794 nm	Mean particle size (nm)
ZVI nanoparticles (analyzed in Milli-Q™ water)	1.29 (0.09)	16.2 (2.85)	27.9 (1.70)	28.0 (2.59)	14.6 (0.28)	10.3 (2.04)	457 (64.0)
ZVI nanoparticles (analyzed in river water)	1.33 (0.46)	7.02 (0.80)	22.7 (1.29)	41.6 (1.00)	18.6 (1.68)	7.4 (0.67)	460 (35.7)
Material	0–46 nm	46–140 nm	140–243 nm	243–424 nm	424–1290 nm	1290–3925 nm	Mean particle size (nm)
River water colloidal particles	1.44 (0.18)	9.57 (0.71)	7.28 (0.56)	13.8 (1.82)	52.2 (0.58)	15.74 (3.25)	860 (57.3)
Material	0–279 nm	279–1373 nm	1373–3047 nm	3047–4538 nm	4538–6760 nm	6760–10,069 nm	Mean particle size (nm)
ZVI microparticles	0(0)	2.16 (0.55)	23.4 (5.03)	37.6 (4.23)	24.0 (6.25)	2.72 (1.69)	3947 (353)

Values in parentheses are standard deviation, $n = 3$.

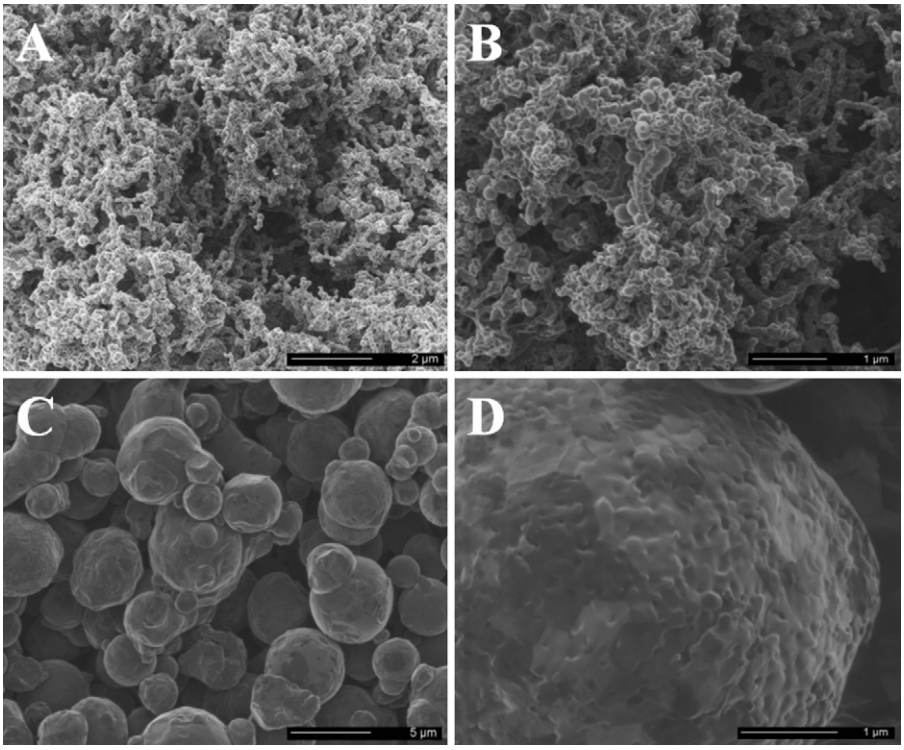

Fig. 1. Focused Ion Beam (FIB) images of: (A) synthesized ZVI nanoparticles (2 μm scale), (B) synthesized ZVI nanoparticles (1 μm scale), (C) Alfa Aesar ZVI microparticles (5 μm scale) and (D) Alfa Aesar ZVI microparticles (1 μm scale).

The bulk chemical composition of nanoparticles was determined by HR-ICP-MS, whilst surface chemistry was analyzed by XPS. In agreement with previous studies, the nanoparticle surfaces were enriched with B, Na and S, with molar% surface values of 5.8%, 1.2% and 0.7%, respectively, and total values, determined with ICP-MS, of 26.6%, 0.3% and 0.4% [8,18].

X-Ray Diffraction (XRD) analysis of the ZVI nanoparticles showed broad peaks relating to poor crystallinity. The dominant phase was metal iron (Fe^0), illustrated by broad diffraction peaks situated at 44.9° and 65° 2-theta.

3.2. River water chemistry

River water was slightly alkaline (pH 8.5) and pH in microcosms containing river water or river water and ZVI microparticles remained constant during experiments (Fig. 2B). Addition of nanoparticles reduced the pH from 8.5 to 8.1 over the 36 days. This was unexpected, as the oxidation of metallic iron, by its reaction with oxygen and water, should increase pH. In the sterile microcosm, the addition of nanoparticles led to an increase in pH, from 8.5 to 8.9, suggesting that the decrease in pH in non-sterile river water may have been due to increased microbial growth and activity, leading to the production of organic acids.

The ORP of the sampled river water (~200 mV) did not change significantly in microcosms containing only river water and river water plus microparticles (Fig. 2C), but decreased after addition of nanoparticles, to −281 mV after 1 day. A highly reducing environment (ORP < 0) was likely created through the rapid consumption of oxygen and other potential oxidants and production of hydrogen [19]. However, the ORP recovered quickly, and almost returned to initial values by day 3. Rapid consumption of oxygen in the presence of ZVI nanoparticles was reflected in a rapid decrease in DO concentration, from 8.2 mg/L (0.51 mM) to 0.6 mg/L (0.038 mM) after 1 day (Fig. 2D). DO concentration subsequently increased slowly during further incubation, only returning to its original concentration after 36 days.

3.3. Bacterial counts

Viable cell abundance increased within 1 day of the start of the experiment in all microcosms and did not change significantly during subsequent incubation in microcosms containing river water and river water plus ZVI microparticles, with only minor fluctuations (Fig. 2A). Similarly, total cell counts (DAPI staining) did not change significantly during the experiment. Culturable bacterial cells on nutrient agar represented approximately 0.2% of the total cells in the river water. In microcosms containing ZVI nanoparticles, the increase in viable cell abundance, although initially smaller than in control microcosms after incubation for 1 day, continued until day 6, and was associated with the decrease in river water pH (Fig. 2). After day 6, viable bacterial counts declined and by day 36 were similar to those in river water microcosms and those containing microparticles. Viable and total cell abundances showed similar patterns, with a large increase in total cell counts in nanoparticle-amended microcosms after day 1. Although the initial chemical oxidation of the ZVI nanoparticles (Fe^0) to ferrous iron (Fe^{2+}) may have had a negative effect on the bacterial population [5–7], subsequent increased total cell abundance may have resulted from growth of iron oxidizing bacteria, gaining energy from oxidation of the resultant ferrous iron to ferric iron (Fe^{3+}). At a pH > 5 the chemical oxidation of Fe^{2+} to Fe^{3+} occurs rapidly and spontaneously [20], with a half-life of <15 min in fully aerated freshwater at pH 7 [21]. Under these conditions iron oxidizing bacteria may find it difficult to compete with the chemical oxidation. However, at low oxygen concentrations, like those created after the addition of ZVI nanoparticles, the chemical oxidation of Fe^{2+} is significantly slower [22]. Biological Fe^{2+} oxidation can take place even under oxygen-poor conditions and the complete oxidation of ZVI nanoparticles to Fe^{3+} may have limited subsequent growth, leading to a decrease in

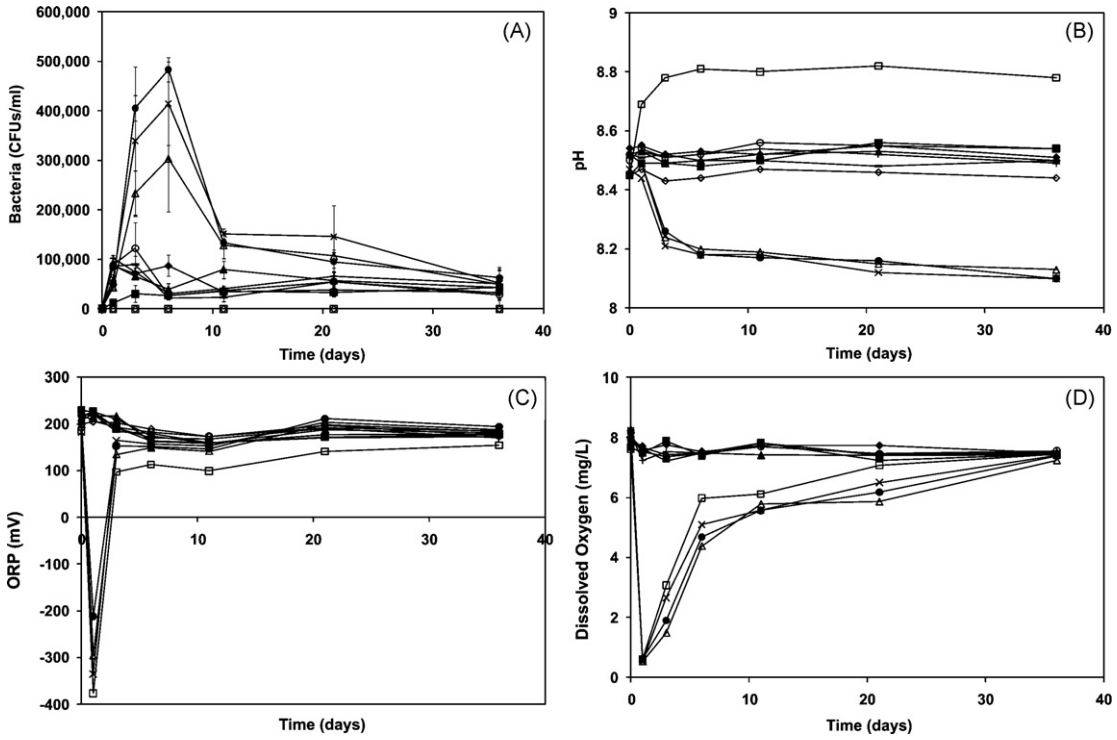

Fig. 2. Changes in viable bacterial counts and river water chemistry during incubation of microcosms for 36 days. (A) Heterotrophic plate counts, (B) pH, (C) oxidation–reduction potential, (D) dissolved oxygen concentration [River Water 1 (–♦–), River Water 2 (–■–), River Water 3 (–▲–), River Water plus Nanoparticles 1 (–×–), River Water plus Nanoparticles 2 (–△–), River Water plus Nanoparticles 3 (–●–), River Water plus Microparticles 1 (—|—), River Water plus Microparticles 2 (▬), River Water plus Microparticles 3 (–○–), Sterile River Water (–◇–), Sterile River Water plus Nanoparticles (–□–)]. Error bars for heterotrophic plate counts are 1× SD (n = 3).

cell abundances. Nevertheless, known iron oxidizers are autotrophs and increased viable cell abundance is likely to have resulted from enhanced growth of heterotrophs, possibly through iron adsorption of both nutrients and bacterial cells [5]. Once these concentrated nutrients had been depleted, the bacterial population could no longer be sustained and so numbers of viable cells subsequently dropped.

The lack of toxicity of the ZVI nanoparticles may have been due to their rapid corrosion and surface oxidation in the highly oxygenated river water (8.2 mg/L; 0.51 mM). A reduction in ZVI nanoparticle toxicity in oxygenated conditions attributed to these factors has been previously reported [6]. In addition, the presence of organic acids in the river water may have mitigated nanoparticle toxicity [23]. Finally, previous studies have only looked at the short-term effects of ZVI nanoparticles (5 min to 1 h) on bacterial cells [5–7]. The longer-term impact of these particles and bacterial recovery or growth after particle oxidation has not previously been investigated. No bacterial growth occurred on plates inoculated with samples from sterile river water microcosm, indicating that the addition of ZVI nanoparticles did not introduce bacteria into the microcosms and that no cross-contamination occurred during the experiment.

3.4. Community structure

Ager et al. [10] assessed the effects of dosing different concentrations of the model organic pollutant pentachlorophenol on bacterial communities in aquatic microcosms and found dose-dependent recovery in bacterial community characteristics, including structure, richness, composition, and taxon turnover, which were used as measures of environmental assessment and biological integrity. A similar approach was adopted in this study to assess the effects of dosing river water with ZVI nanoparticles or microparticles, using DGGE analysis of amplified 16S rRNA gene fragments to characterize bacterial communities (see Figs. S1–S3, Supporting Information). DGGE band richness and intensity were used to infer richness and relative abundance of bacterial taxa [13] and the mean slope values of rank-abundance plots were used as a descriptive statistic of evenness, with perfect evenness represented by zero (Fig. 3A). No significant change in community structure was observed in any of the microcosms (Table 2), but addition of nanoparticles, but not microparticles, led to a decrease in richness, which decreased from 42.0 ± 1.0 on day 0 to 35.7 ± 2.5 at day 1, subsequently returning to initial values after day 3.

Changes in bacterial community composition were examined using two complementary approaches: total compositional change, representing the similarity (Sørenson index) of each sample with the original pre-perturbation (day 0) sample (Fig. 3C), and sequential compositional change, representing the similarity (Sørenson index) of each sample with the sample from the preceding sampling point (Fig. 3D). Both ZVI nanoparticles and microparticles had a large impact on composition with a mean difference in similarity of 64.3 ± 7.5% between days 0 and 1 for microcosms dosed with nanoparticles, and 67.0 ± 5.0% for those dosed with microparticles (Fig. 3C). Community composition subsequently recovered (Table 2). In addition, similarity in the control microcosms decreased in a similar manner over time, reflecting the normal dynamic behaviour of natural communities (10). In the microcosms dosed with ZVI nanoparticles similarity varied on average by 31.9 ± 7.9% from one time point to the next (Fig. 3D), with similar values (34.7 ± 8.1% and 36.2 ± 8.1%, respectively) for ZVI microparticle and control microcosms. The level of sequential variation in similarity did not correlate with perturbation and was not significantly different across the three experimental conditions (ANOVA: $F_{2,51}$ = 1.03; P = 0.363).

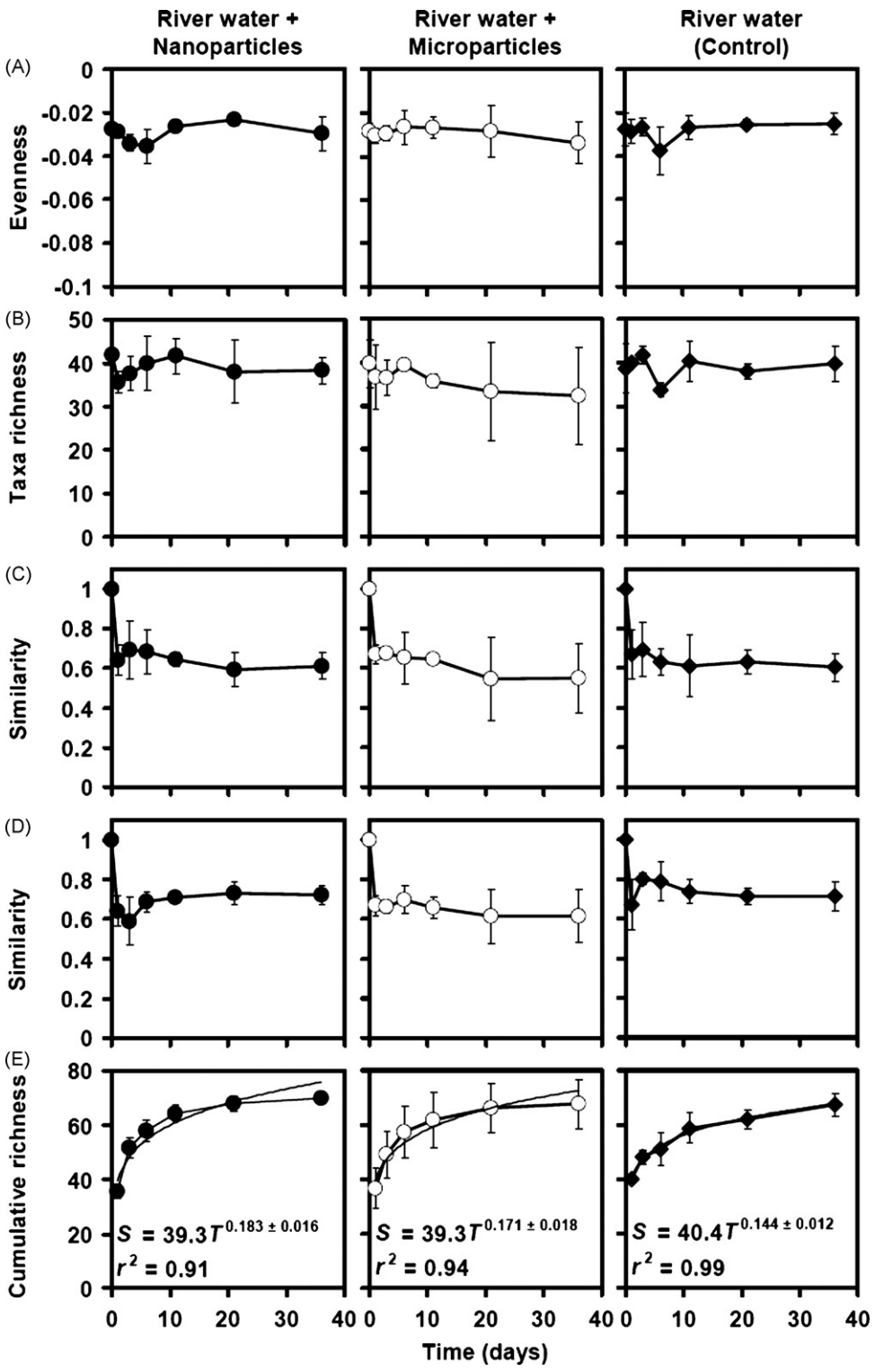

Fig. 3. Changes in bacterial community characteristics in river water microcosms under different treatments [nanoparticles (closed circles), Microparticles (open circles) and river water only (closed diamonds)] during incubation period of 36 days. (A) changes in structure (evenness) using the mean slope values from rank-abundance plots; (B) taxa richness; (C) total compositional change; (D) sequential compositional change; and (E) taxa–time relationships. Also given for (E) are the taxa–time power law equation, $S = cT^w$. All regression coefficients were significant ($P < 0.0001$). Error bars represent the standard deviation of the mean ($n = 3$ in all cases).

Temporal turnover of bacterial taxa across the treatments was assessed using taxon–time relationships (TTR), which describe how the observed taxon richness of a community in a habitat of fixed size increases with the length of time over which the community is monitored [13]. The TTR can be modelled with the power law equation, $S = cT^w$, where S is the cumulative number of observed taxa over time T, c is the intercept and w is the slope of the line or temporal scaling exponent such that increasing values of w reflect greater rates of turnover. An increase in turnover would be expected following a perturbation or environmental stress [10,13]. However, the mean temporal scaling exponents did not increase with disturbance (Fig. 3E) and the mean values of slopes

Table 2
ANOVA test results comparing community structure, taxon richness and community similarity in samples taken from microcosms containing untreated river water and containing river water treated with microparticles or nanoparticles at the times indicated against pre-perturbation values ($t = 0$).

	Day	River water + nanoparticles		River water + mi croparticles		River water (control)	
		F	*P*	*F*	*P*	*F*	*P*
Community structure	1	0.53	0.507	0.53	0.507	0.04	0.856
	3	7.14	0.056	0.15	0.716	0.05	0.841
	6	3.22	0.147	0.18	0.693	1.76	0.256
	11	0.39	0.566	0.15	0.717	0.04	0.856
	21	5.28	0.083	0.001	0.964	0.22	0.667
	36	0.17	0.701	0.85	0.409	0.22	0.662
Taxon richness	1	16.41	0.015*	0.32	0.602	0.16	0.71
	3	3.25	0.146	0.71	0.446	0.74	0.439
	6	0.3	0.613	0.01	0.923	2.16	0.215
	11	0.02	0.896	1.47	0.292	0.16	0.714
	21	0.91	0.395	0.77	0.43	0.04	0.855
	36	3.9	0.119	1.03	0.368	0.06	0.816
Community similarity	1	67.82	0.001	130.14	0.0001*	20.5	0.001*
	3	13.23	0.022	517.13	0.0001*	15.15	0.018*
	6	23.89	0.008	20.39	0.011*	88.27	0.001*
	11	344.98	0.0001	563.32	0.0001*	18.53	0.013*
	21	67.26	0.001	13.73	0.021*	108.37	0.0001*
	36	98.31	0.001	19.96	0.011*	91.63	0.001*

Given are the *F*-test statistics and significance (*P*). Degrees of freedom = 1.4 in all instances.
* The relationships that were significantly different from day 0 at the $P < 0.05$ level.

were not significantly different across treatments (control versus ZVI microparticles: $t = 1.14$, d.f. = 8, $P = 0.214$; control versus ZVI nanoparticles: $t = 1.35$, d.f. = 8, $P = 0.289$; ZVI nanoparticles versus ZVI microparticles: $t = 0.35$, d.f. = 8, $P = 0.730$); that is the application of ZVI nano- or microparticles did not produce a significant increase in cumulative taxon richness.

4. Conclusions

This is the first study on the impact of ZVI nanoparticles on a natural river water bacterial community. ZVI nanoparticles synthesized by $NaBH_4$ reduction have been extensively characterized and their impact on river water pH, ORP and DO concentration monitored over a 36-day period. This study highlights how ZVI nanoparticles aggregate in near-neutral pH environmental samples. Despite this aggregation, the nanoparticles were more reactive than their microscale counterparts, leading to much greater decreases in solution ORP and DO concentration. However, the rapid and intense change in these chemical parameters was only temporary, returning to pre-treatment values over the experimental period, as the nanoparticles oxidized.

Despite studies reporting the cytotoxic nature of ZVI nanoparticles at low concentrations (<100 mg/L) [5–7], results of this 36-day study indicate that the addition of 100 mg/L ZVI nanoparticles to aerobic river water was not toxic to the indigenous river water bacterial community. Although the addition of ZVI nanoparticles led to an initial decrease in bacterial community richness and inhibited the increase in viable cell counts observed in the control and ZVI microparticle amended microcosms, the community richness returned to initial values after day 3 and over the experimental period the presence of these particles led to an increase in total cell abundance. Importantly, no statistically significant change in bacterial community structure or composition was observed in the presence of these nanoparticles.

However, it has previously been shown that the toxicity effects of ZVI nanoparticles increase with concentrations ranging from 0.1 to 10 g/L [5]. In addition, previous work carried out by Barnes et al. [24], showed that the addition of ZVI nanoparticles was inhibitory to the biological reduction of TCE and sulphate in contaminated groundwater, under anaerobic conditions. An effect was seen with concentrations as low as 0.01 g/L, but complete inhibition and a decrease in viable bacterial numbers was only observed at concentrations of 0.3 g/L or higher [24]. An inhibitory effect of biological dechlorination in the presence of 1 g/L ZVI nanoparticles has also recently been reported elsewhere [25]. Therefore, information from studies investigating the impact of ZVI nanoparticles on bacteria highlight that toxicity is dose- and species-dependent, and is highly affected by environmental conditions. Therefore all these factors need to be considered before the toxicity of ZVI nanoparticles can be fully understood.

Supporting information

The supporting information shows the DGGE gels of bacterial 16S rRNA genes amplified from river water microcosms with and without addition of ZVI nanoparticles or microparticles sampled after incubation for 0, 1, 3, 6, 11, 21 and 36 days ($n = 3$).

Acknowledgements

Research was supported by NERC. The authors also thank Andrew Whiteley, CEH Oxford, for training and use of the epifluorescence microscope and José Ángel Siles López, University of Córdoba, for assistance with river water sampling.

Appendix A. Supplementary data

Supplementary data associated with this article can be found, in the online version, at doi:10.1016/j.jhazmat.2010.08.006.

References

[1] F. Li, C. Vipulanandan, K.K. Mohanty, Microemulsion and solution approaches to nano-scale particle iron production for degradation of trichloroethylene, Colloids Surf. A 223 (2003) 103–112.
[2] S. O'Hara, T. Krug, J. Quinn, C. Clausen, C. Geiger, Field and laboratory evaluation of the treatment of DNAPL source zones using emulsified zero-valent iron, Rem. J. 16 (2006) 35–56.
[3] D.W. Elliott, W. Zhang, Field assessment of nanoscale bimetallic particles for groundwater treatment, Environ. Sci. Technol. 35 (2001) 4922–4926.
[4] R. Glazier, R. Venkatakrishnan, F. Gheorghiu, L. Walata, R. Nash, W.X. Zhang, Nanotechnology takes root, Civ. Eng. 73 (2003) 64–69.

[5] M. Diao, M. Yao, Use of zero-valent iron nanoparticles in inactivating microbes, Water Res. 43 (2009) 5243–5251.
[6] C. Lee, J.Y. Kim, W.I. Lee, K.L. Nelson, J. Yoon, D.L. Sedlak, Bactericidal effect of zero-valent iron nano-scale particles on Escherichia coli, Environ. Sci. Technol. 42 (2008) 4927–4933.
[7] M. Auffan, W. Achouak, J. Rose, M.-A. Roncato, C. Chaneac, D.T. Waite, A. Masion, J.C. Woicik, M.R. Wiesner, J.-V. Bottero, Relation between the redox state of iron-based nanoparticles and their cytotoxicity toward Escherichia coli, Environ. Sci. Technol. 42 (2008) 6730–6735.
[8] R.J. Barnes, O. Riba, M.N. Gardner, T.B. Scott, S.A. Jackman, I.P. Thompson, Optimization of nano-scale nickel/iron particles for the reduction of high concentration chlorinated aliphatic hydrocarbon solutions, Chemosphere 79 (2010) 448–454.
[9] S. Saby, I. Sibille, L. Mathieu, J.L. Paquin, J.C. Block, Influence of water chlorination on the counting of bacteria with DAPI (4′,6-diamidino-2-phenylindole), Appl. Environ. Microbiol. 63 (1997) 1564–1569.
[10] D. Ager, S. Evans, H. Li, A.K. Lilley, C.J. van der Gast, Anthropogenic disturbance affects the structure of bacterial communities, Environ. Microbiol. 12 (2010) 670–678.
[11] G. Muyzer, E.C. De Waal, A.G. Uitterlinden, Profiling of complex microbial populations by denaturing gradient gel electrophoresis analysis of polymerase chain reaction-amplified genes coding for 16S rRNA, Appl. Environ. Microbiol. 59 (1993) 695–700.
[12] G.W. Nicol, D. Tscherko, T.M. Embley, J.I. Prosser, Primary succession of soil Crenarchaeota across a receding glacier foreland, Environ. Microbiol. 7 (2005) 337–347.
[13] C.J. van der Gast, D. Ager, A.K. Lilley, Temporal scaling of bacterial taxa is influenced by both stochastic and deterministic ecological factors, Environ. Microbiol. 10 (2008) 1411–1418.
[14] A.K. Lilley, J.C. Fry, M.J. Bailey, M.J. Day, Comparison of aerobic heterotrophic taxa isolated from four root domains of mature sugar beet (Beta vulgaris), FEMS Microbiol. Ecol. 21 (1996) 231–242.
[15] J. Fowler, L. Cohen, P. Jarvis, Practical Statistics for Field Biologists, John Wiley and Sons, Chichester, UK, 1998.
[16] L. Zhang, A. Manthiram, Chains composed of nanosize metal particles and identifying the factors driving their formation, Appl. Phys. Lett. 70 (1997) 2469–2471.
[17] T. Phenrat, N. Saleh, K. Sirk, R. Tilton, G.V. Lowry, Aggregation and sedimentation of aqueous nanoiron dispersions, Environ. Sci. Technol. 41 (2007) 284–290.
[18] B. Schrick, J.L. Blough, A.D. Jones, T.E. Mallouk, Hydrodechlorination of trichloroethylene to hydrocarbons using bimetallic nickel–iron nano-scale particles, Chem. Mater. 14 (2002) 5140–5147.
[19] W. Zhang, Nanoscale iron particles for environmental remediation: an overview, J. Nanopart. Res. 5 (2003) 323–332.
[20] H.L. Ehrlich, Geomicrobiology, Marcel Dekker, Inc., New York, NY, 1990.
[21] W. Stumm, J.J. Morgan, Aquatic Chemistry, 2nd ed., John Wiley & Sons, New York, NY, 1981.
[22] L. Liang, J.A. McNabb, J.M. Paulk, B. Gu, J.F. McCarthy, Kinetics of Fe(II) oxygenation at low partial pressure of oxygen in the presence of natural organic matter, Environ. Sci. Technol. 27 (1993) 1864–1870.
[23] J. Fabrega, J.C. Renshaw, J. Lead, Interactions of silver nanoparticles with Pseudomonas putida biofilms, Environ. Sci. Technol. 43 (2009) 9004–9009.
[24] R.J. Barnes, O. Riba, M.N. Gardner, A.C. Singer, S.A. Jackman, I.P. Thompson, Inhibition of biological TCE and sulphate reduction in the presence of iron nanoparticles, Chemosphere 80 (2010) 554–562.
[25] Z. Xiu, Z. Jin, T. Li, S. Mahendra, G.V. Lowry, P.J.J. Alvarez, Effects of nano-scale zero-valent iron particles on a mixed culture dechlorinating trichloroethylene, Bioresour. Technol. 101 (2010) 1141–1146.